

Copyright

by

Tong Ren

2013

**The Thesis Committee for Tong Ren  
Certifies that this is the approved version of the following thesis:**

**The role of the Mexican Plateau in shaping rainfall over Texas**

**APPROVED BY  
SUPERVISING COMMITTEE:**

**Supervisor:**

---

Rong Fu

---

Robert E. Dickinson

---

Zong-Liang Yang

**The role of the Mexican Plateau in shaping rainfall over Texas**

**by**

**Tong Ren, B.S., M.S.**

**Thesis**

Presented to the Faculty of the Graduate School of

The University of Texas at Austin

in Partial Fulfillment

of the Requirements

for the Degree of

**Master of Science in Geological Sciences**

**The University of Texas at Austin**

**December 2013**

## **Acknowledgements**

The GRACE land data used in this study were processed by Sean Swenson and supported by the NASA MEaSUREs Program. The data are available at <http://grace.jpl.nasa.gov>. The GPCP Precipitation data used in this study were provided by the NOAA/OAR/ESRL PSD, Boulder, Colorado, USA, from their Web site at <http://www.esrl.noaa.gov/psd/>. This work is supported by the National Science Foundation (NSF) AGS-0937400.

## **Abstract**

### **The role of the Mexican Plateau in shaping rainfall over Texas**

Tong Ren, M S Geo Sci

The University of Texas at Austin, 2013

SUPERVISOR: Rong Fu

Previous studies have suggested that advection from the Mexican Plateau (MP) may influence rainfall over Texas in spring and summer; generally air ascends over the cordillera and descends over the southern plains. The two mechanisms may link the northern Mexico drought to Texas drought. Observations and the Community Earth System Model are used in this study to describe the 2011 Texas-northern-Mexico drought and examine the role of the MP on the hydro-climate over the southern US, providing implications for the linkage between the MP and rainfall over Texas. A control run and three experimental runs were performed with prescribed sea surface temperatures and sea ice fractions. The results show that when the MP becomes dry, rainfall declines locally and downstream. During the spring, the dry air brought to Texas by prevailing westerly winds suppresses local convection; but dry air advection from the highlands has little influence on rainfall over Texas during the summer when Texas is no longer in the downstream areas. During the summer, a warmer MP draws moist air over the peripheral low elevation areas to the highlands; it bends the low-level jet towards the highlands and an anti-cyclonic flow anomaly forms over the southern US, which causes air to diverge and tends to reduce rainfall over the southern US.

## Table of Contents

List of Tables .....	vii
List of Figures .....	viii
Chapter 1: Introduction .....	1
Chapter 2: Methodology .....	5
Chapter 3: Observations of the 2011 Texas Drought.....	9
Chapter 4: Model Results.....	13
4.1 Moisture transport and 850 hPa air divergence .....	13
4.2 Potential temperature and meridional wind speed .....	15
4.3 Rainfall.....	16
Chapter 5: Conclusions .....	18
References.....	36

## **List of Tables**

Table 1:	Experiments design.....	20
----------	-------------------------	----

## List of Figures

Figure 1:	Precipitation rate ( $\text{mm day}^{-1}$ ) simulated by CESM (a) – (f) and observed by TRMM (g) – (l) over $[112^{\circ}\text{W}, 90^{\circ}\text{W}] \times [18^{\circ}\text{N}, 40^{\circ}\text{N}]$ for the spring and summer of 2011.....	21
Figure 2:	850 mb specific humidity ( $\text{g kg}^{-1}$ ) and horizontal wind ( $\text{m s}^{-1}$ ) from CESM (a) – (f) and reanalysis (g) – (l) over $[112^{\circ}\text{W}, 90^{\circ}\text{W}] \times [18^{\circ}\text{N}, 40^{\circ}\text{N}]$ for the spring and summer of 2011.....	22
Figure 3:	Normalized TRMM 3B43 monthly mean precipitation rate anomalies over $[120^{\circ}\text{W}, 80^{\circ}\text{W}] \times [15^{\circ}\text{N}, 38^{\circ}\text{N}]$ in April and July of 2011. ....	23
Figure 4:	GRACE LWET over the south-central United States in April and July of 2011.....	24
Figure 5:	Differences between April 2011 and April 2010 in monthly mean lower and middle troposphere AIRS water vapor mass mixing ratio and NCEP horizontal wind field over the continental US. ....	25
Figure 6:	The same as Figure 5 except for the differences between July 2011 and July 2000.....	26
Figure 7:	Scatter plot of the precipitation rate anomalies ( $\text{mm day}^{-1}$ ) over Texas and the surface air temperature anomalies ( $^{\circ}\text{C}$ ) of the MP in June, July and August, and the linear regression line. ....	27
Figure 8:	850 hPa specific humidity ( $\text{g kg}^{-1}$ ) and horizontal wind field differences between E1 and CTRL during spring and summer.....	28
Figure 9:	The same as Fig. 8 except for the differences between E2 and CTRL.	29



Figure 10:	700 hPa air divergence ( $\text{day}^{-1}$ ) differences between E2 and CTRL during spring and summer. The solid contours represent the air divergence tendency whereas the dashed contours represent the air convergence tendency. ....	30
Figure 11:	Vertical cross sections of potential temperature (K, shadings), meridional wind ( $\text{m s}^{-1}$ , contours), and zonal wind ( $\text{m s}^{-1}$ , white arrows) along $30^{\circ}\text{N}$ from $120^{\circ}\text{W}$ to $80^{\circ}\text{W}$ for spring (MAM). The contours show meridional wind speed for CTRL and differences in meridional wind speed between the experiment runs and the control run for E1, E2, and E3. ....	31
Figure 12:	The same as Fig. 11 except for summer (JJA).....	32
Figure 13:	The 2001-2011 mean seasonal precipitation rate (mm/day) differences between E1 and CTRL during spring (March-May) and summer (June-August).....	33
Figure 14:	The same as Figure 13 except for the differences between E2 and CTRL. ....	34
Figure 15:	The same as Figure 13 except for the differences between E3 and CTRL. ....	35

## **Chapter 1: Introduction**

Droughts have a substantial impact on agriculture and the ecosystem of affected regions. The United States is the world's largest grain-exporting country; it accounts for over half the global export market for corn and nearly half the soybean market. Therefore, an extreme drought in the US not only cost billions of dollars economic losses in US, but also cause considerable disruption of worldwide food supplies that affect people, prices, and political stability worldwide.

In 2011, Texas endured the driest 12-month span on record from October 2010 to September 2011. During the drought some weather stations set records of 100 consecutive days of temperatures higher than 100 degrees Fahrenheit. Widespread wildfires destroyed millions of acres, stock tanks dried up, and trees wilted and turned brown. The brutality of the drought placed local agriculture and livestock in jeopardy. Agriculture losses reached \$7.62 billion (<http://today.agrilife.org/2012/03/21/updated-2011-texas-agricultural-drought-losses-total-7-62-billion/>).

Numerous previous drought studies have tried to link sea surface temperature (SST) variability such as ENSO, the Atlantic Multidecadal Oscillation (AMO), the Interdecadal Pacific Oscillation (IPO) to continental rainfall and surface temperature variability (e.g., Lau et al. 2008; Mo et al. 2009; Zhang et al. 2011; Dai 2012). These analyses can provide SST patterns that favor drought in certain areas. However, numerous other factors can also influence seasonal rainfall, such as aerosols (Menon et al. 2002; Zhao et al. 2012), soil moisture (Dirmeyer 1994; Koster et al. 2004; Brimelow et al. 2011), and topography (Boos and Kuang, 2010). These factors often lead to nonlinear responses to SST variability including seasonal temperature and precipitation

anomalies. Based on Atmospheric Model Intercomparison Project (AMIP) and Coupled Model Intercomparison Project (CMIP) model experiments, Hoerling et al. (2013) revealed that a typical La Niña during October to May is favorable for rainfall deficit over the southern states during the subsequent summer and the associated antecedent dry conditions may closely link to persistent summer heat wave and rainfall deficits. However, they also indicated that although the probability of extremes such as the 2011 Texas drought can be greatly increased in specific SST conditions, random internal variability plays an important role in determining the observed outcomes. Therefore, expending more effort on studying internal variability and interactions within the water cycle may help us improve the ability to predict extreme weather events.

The North American Drought Monitor (NADM) program documents two Texas droughts since 2002, namely the 2006 Texas drought and 2011 Texas drought. The NADM maps of drought conditions are based on a combination of indices including the Palmer Drought Indices, which are measures of dryness that take both temperature and moisture into account. The monthly operational NADM maps show that during the two springs and summers of 2006 and 2011, the MP also experienced severe drought. Thus, we might speculate a link between the spring Texas drought and the spring MP drought as prevailing downslope westerlies and southwesterlies bring warm and dry air from the MP to cap the low level wet air over the plains. This linkage implies the importance of the MP in modulating spring rainfall over Texas.

Myoung and Nielsen-Gammon (2010) indicate that warm air transported from the Rocky Mountains and the MP to Texas contributed to 700 hPa warming during summer. They also suggest that persistent anti-cyclonic anomalies may enhance warm air transport, increasing convective inhibition (CIN). This conclusion was based on a back-trajectory analysis using 56 years of reanalysis data for the month of July. However,

when summer comes, winds are generally southeasterly at 700 hPa over the Gulf of Mexico and northeastern Mexico; southerly over Texas and New Mexico. Their back-trajectory analysis also shows that the dominant source for the 700 hPa air mass over Texas in July was the Gulf of Mexico. Hence, warm air transport from the western high elevation areas in summer may not be significant. Therefore, although their work implies a connection between the high terrain and summer rainfall over Texas, they neglected the effects of the MP on Texas precipitation during the summer within the context of circulation response.

Tang and Peiter (1984) compared meteorological fields over North America to meteorological fields over Tibet, highlighting the plateau monsoon concept. They indicate that the low-level jet (LLJ) over Texas was noticeably affected by the surface energy budget over the Western Plateau and, in addition, relatively high precipitation areas lay on the western side of the LLJ rather than under it. Previous studies have documented the close connection between the LLJ and the development of deep convection (Stensrud, 1996). The diurnal variation of the Great Plains LLJ supports the diurnal variation of rainfall (Mo and Berbery, 2004). The MP is a large arid-to-semiarid plateau that limits the flow of moisture from the eastern tropical Pacific Ocean and the Gulf of California and confines the moisture to the western slope of the MP; at the same time the MP limits the flow of moisture from the Gulf of Mexico and confines the moisture to the eastern slope of the MP.

Based on a general circulation model (GCM) and linear and nonlinear stationary wave model studies, Ting and Wang (2006) show that the dominant factor in maintaining the Great Plains time-averaged LLJ is the MP, which blocks the easterly wind along the southern flank of the North Atlantic Subtropical High (NASH) and causes the flow to turn northward. NASH has been referred as one of the most important factors influencing

the hydrological cycling over the southeastern Great Plains of the US (Li et al., 2012). Westward expansion and enhancement of the NASH can bring large amounts of moisture from the Atlantic Ocean and the Gulf of Mexico to the southern plains. Rainfall over the US southern plains is also significantly correlated with the strength of the Caribbean low-level jet (CLLJ) during the cool season from October to April: a strong CLLJ is associated with increased rainfall over Louisiana and Texas (Cook and Vizio, 2010). Therefore, based on the aforementioned studies, the MP can affect rainfall over Texas by interacting with NASH and modulating LLJ.

To the best of our knowledge, no numerical simulations have been conducted to study how the MP affects rainfall over Texas. Therefore, to gain insight into the role of the MP in shaping rainfall over Texas, we use the Community Earth System Model (CESM) 1.0.4 (Hurrell et al., 2013) to investigate how the MP affects rainfall over the southern plains, i.e. the interactions among the MP, large-scale circulations, and precipitation. These model experiments aim at gaining a better understanding of the influence of surface water and energy budgets of the MP on rainfall over Texas. We hope the experiments would further our understanding on whether MP drought can exacerbate Texas drought.

## **Chapter 2: Methodology**

Satellite observations and reanalysis data were used in this study to show rainfall, terrestrial water storage, atmospheric water vapor content, and wind field during the 2011 Texas-northern-Mexico drought. The Tropical Rainfall Measuring Mission (TRMM) 3B43 version 7 monthly mean precipitation rate data were used to show rainfall conditions during the spring and summer of 2011 and 2010, respectively. The Gravity Recovery and Climate Experiment (GRACE) Release 05 monthly liquid water equivalent thickness (LWET) data (Landerer and Swenson, 2012) were used to show the monthly terrestrial water storage anomalies during the spring and summer of 2011. The Atmospheric Infrared Sounder (AIRS) water vapor mass mixing ratio (WVMMR) product and the National Centers for Environmental Prediction (NCEP) National Center for Atmospheric Research (NCAR) reanalysis data (Kalnay et al. 1996) were used to show changes in water vapor content and horizontal wind field between 2011 and 2010, respectively. The TRMM 3B43 data and the NCEP/NCAR reanalysis were also used to evaluate the performance of CESM on low-level circulations and rainfall over the Mexican Plateau and Texas. The Global Precipitation Climatology Project (GPCP) Version 2.2 Combined Precipitation Data Set (Adler et al. 2003) and the NCEP/NCAR reanalysis were used to study the statistical relationship between the surface air temperature of the MP and rainfall over Texas during the summer.

In 2011, the MP was also hit hard by drought. The National Oceanic and Atmospheric Administration (NOAA) North American Drought Monitor maps show that the drought over MP started from the March 2011 and lasted more than one year; during the spring and summer of 2011, D3 drought (extreme drought) and D4 drought (exceptional drought) were present over large portions of the MP, especially the northern

MP. Therefore, it is reasonable to hypothesize that the drought over MP may be linked to the drought over Texas. We first integrated the CESM from 2000 to 2011 using observed SST, and then compared the model results with observations. The results show that the CESM cannot realistically simulate the 2011 Texas-northern-Mexico drought, although the precipitation patterns of the model and the observation are analogous. As showed in Fig. 1, compared with the TRMM observation, CESM overestimates the precipitation rate over the Mexican Plateau and Texas during the spring and summer of 2011. The precipitation rates from the CESM simulation are about  $3 \text{ mm day}^{-1}$  over the southern Mexico Plateau during the spring, but the precipitation rates from the TRMM data are almost  $0 \text{ mm day}^{-1}$  over the Mexican Plateau. The precipitation rate from CESM exceeds  $15 \text{ mm day}^{-1}$  over the Sierra Madre del Sur in August, but the precipitation rate from the TRMM data is less than  $8 \text{ mm day}^{-1}$  over the same area. As showed in Fig. 2, the differences in low-level moisture and horizontal winds between the CESM simulation and the NCEP/NCAR reanalysis are smaller than the differences in rainfall. Compared with the NCEP/NCAR reanalysis, CESM underestimates the specific humidity over the southern Mexican Plateau during the summer. Due to the inability to generate a “real” 2011 Texas-northern-Mexico drought, we artificially dry and warm the Mexican Plateau in the following CESM experiments to study the general impacts of the MP on circulation and rainfall over Texas.

With knowledge of actual 2011 Texas drought conditions obtained from satellite observations, we used the CESM to conduct a control simulation (CTRL) and three experimental simulations (E1, E2, and E3), to test the surface water and energy budgets of the MP in shaping rainfall over Texas. These simulations do not aim to create a Texas drought as observed but focus on impacts of the MP on circulation and rainfall over Texas. Forcing by natural variability is eliminated by prescribing the Hadley Center

optimally interpolated climatological SST and sea-ice fraction data. Over land, the Community Atmosphere Model (CAM5) was coupled to the Community Land Model (CLM4); the sea ice component in these experiments was the Community Ice Code (CICE4). The experiments were integrated for 12 years at a spatial resolution of 0.9° latitude by 1.25° longitude and a time step of 30 minutes. We discarded the first year of the integration for model spin-up and averaged the data from the last 11 years to get the model climatology.

We first determined the grid points within  $[112^{\circ}\text{W}, 95^{\circ}\text{W}] \times [15^{\circ}\text{N}, 30^{\circ}\text{N}]$  where the surface geopotential is greater than  $6000 \text{ m}^2/\text{s}^2$ . These grid points defined the MP in our experiments. Dryness and hotness, the two fundamental features of drought, are produced over the MP in the experimental runs. In E1, we dried up the MP by fixing the soil water to a small constant value. At each time step, we set the soil liquid water of each layer to 0.2 mm and the water in the unconfined aquifer to 4000 mm, and we let the subsurface runoff account for the water change within the soil column. Thus, the soil over the MP is always dry and the resultant water table is always below the lower boundary of the active soil layers. In E2, we set the direct and diffusive albedos of the MP to zero for both visible and infrared wavebands. For vegetation areas in CLM4, we changed vegetation albedos to zero; for non-vegetation areas in CLM4, we changed ground albedos to zero. Thus, since more solar radiation is absorbed by the land surface during the daytime, the surface temperature of the MP increases, producing a warmer MP. The monthly mean surface temperatures of the MP are about 1-3 K higher in E2 than in CTRL during the spring and summer (The figure is not shown here); the monthly mean daily maximum temperatures of the MP are about 6-8/4-6 K higher in E2 than in CTRL during the spring/summer (The figure is not shown here). In E3, a dry and warm MP was



created using the same methods as in E1 and E2. These experiments are documented in Table 1.

### **Chapter 3: Observations of the 2011 Texas Drought**

During the drought, the rainfall deficit began in the late fall through winter of 2010, and the deficit was most pronounced in the spring and summer of 2011 because most of the rainfall is normally received during these two seasons. Fig. 3 shows the TRMM 3B43 version 7 monthly mean precipitation rate anomalies over  $[120^{\circ}\text{W}, 80^{\circ}\text{W}] \times [15^{\circ}\text{N}, 38^{\circ}\text{N}]$  in April and July of 2011. The monthly mean precipitation rates from 1998 to 2012 were used to derive the climatological seasonal cycle of the precipitation rate. This was subtracted from the 2011 data to obtain the seasonal cycle of the anomalous precipitation rate for 2011, which was then normalized by the climatological mean seasonal cycle. From the normalized precipitation patterns of 2011, we can see that less rain fell over the Mexican Plateau and Texas throughout the spring and summer of 2011.

Previous studies show that the positive soil moisture-precipitation feedback could further aggravate Texas drought by modulating surface conditions (Myoung and Nielsen-Gammon, 2010). Therefore, here we report on satellite observations of soil and lower atmosphere moisture during the 2011 Texas drought. During the drought, extreme low moisture content underneath the land surface was detected by GRACE. Fig. 4 shows the distribution of the GRACE (Release 05) monthly LWET over Texas in April and July of 2011. We derived the climatological seasonal cycle of LWET from the 2004-2010 GRACE data, and subtracted this seasonal cycle from the 2011 data to obtain the monthly LWET anomalies for the spring and summer of 2011. Fig. 4 shows strong negative LWET anomalies underneath Texas during the spring and summer of 2011, which refers to severe dry soil conditions during the drought.

The severe soil water deficit was not associated with low water vapor content for all months during the spring and summer in the lower troposphere. Compared to 2010,

the 2011 spring and summer lower troposphere water vapor content was lower in May, June, and August but higher in March and July. In April 2011, a strong time-mean LLJ brought abundant moisture from the Gulf of Mexico to low-elevation areas of Texas; at the same time, westerlies prevailed over northern portions of the MP and southwesterlies prevailed over northeastern portions of the MP. In July 2011, wind over northern Mexico blew northwestward; over Texas, the lower troposphere water vapor concentration was high. Fig. 5 shows the differences between April 2011 and April 2010 in monthly mean lower and middle troposphere AIRS water vapor mass mixing ratio (WVMMR) over the Mexican Plateau and Texas. Fig. 6 is the same as Fig. 5 except for the differences between July 2011 and July 2000. The WVMMR on an isobaric surface shown in the two figures refers to the WVMMR between this pressure level and the lower level. For example, the 850 mb WVMMR in these figures stands for the WVMMR within the layer bounded by the 925 mb and 850 mb isobaric surfaces; the 925 mb WVMMR represents the WVMMR below the 925 mb isobaric surface.

Fig. 5 shows that the lower and middle troposphere WVMMR over the MP during April of the drought year was significantly lower than during April of a normal year. Between 700 mb and 850 mb, the WVMMR over northeastern portions of the MP in April 2011 was about  $2 \text{ g kg}^{-1}$  lower than in April 2010. Fig. 5 also shows that water vapor content below 925 mb over Texas during the drought year was higher than during a normal year, whereas water vapor content between 700 mb and 850 mb during the drought year was lower than during the normal year. The results suggest that in April 2011, the dry air brought by strong prevailing westerlies from the MP to Texas dried 700 mb.

In the summer of 2011, however, air over the MP was not uniformly drier than in a normal year summer. This was because the wind field changed direction as the summer

came, i.e. during the summer humid air was brought by southeasterlies from the Gulf of Mexico to the Mexican highlands. As shown in Fig. 6, the WVMMR between 600 mb and 850 mb over most parts of the northern MP in July of 2011 was even higher than in July of 2010. Fig. 6 also shows that water vapor content between the surface and the middle troposphere in July 2011 was higher than in July 2010, particularly between 700 mb and 850 mb. Since the wind field over the northern MP changed from westerlies in spring to southerlies in summer, almost no dry air was transported from the western highlands to Texas during the summer, or at least the westerly dry air advection was not significant. Therefore, unlike in the findings of Myoung and Nielsen-Gammon (2010) regarding the impact of dry air advection on convection over Texas during summer, we find that such westerly dry air advection did not prevail during the summer of 2011. This leads us to question whether the role of westerly dry air advection on summer convection over Texas is overemphasized in Myoung and Nielsen-Gammon (2010).

In spite of a sufficient supply of water vapor, Texas was still hit hard by drought in July 2011 as showed in Fig. 3 and 4. Another recent study suggests that the drought continuation into the summer of 2011 was not significantly SST-forced and is presumably attributed to internal atmospheric variability or soil moisture-precipitation feedback (Seager et al. 2013). Generally in July, air ascends over the cordillera and descends over the central United States and Texas, and the descending air is concentrated at low levels over Texas (Barlow et al. 1998). We argue that one source of internal atmospheric variability might be the precipitation response over Texas to the surface energy budget of the MP. Fig. 7 shows the statistical relationship between surface air temperature anomalies of the MP and precipitation rate anomalies over Texas during June, July, and August. We averaged the NCEP/NCAR reanalysis monthly surface air temperature over the MP and the GPCP version 2.2 combination precipitation rate over

Texas. Then we removed their linear trends and seasonal cycles to derive the time series of the surface air temperature anomalies of the MP and the precipitation rate anomalies over Texas. Fig. 7 shows a scatter plot of 97 samples collected in June, July and August from January 1979 to June 2011 and the linear regression line. The surface air temperature anomalies of the MP is moderately anti-correlated with the precipitation rate over Texas, i.e. during summer, a warmer MP is associated with decreased rainfall over Texas whereas a cooler MP is associated with increased rainfall over Texas. The correlation coefficient is -0.3584, which is 99% statistically significant. Hence, about 10% of the summer rainfall variation over Texas can be explained by the summer temperature variation over the Mexican Plateau. A possible underlying mechanism is that during summer, the warm low above a warmer MP drags air from ambient low elevation areas to highlands, which is favorable for an air divergence tendency over Texas that can stabilize the lower atmosphere.

## Chapter 4: Model Results

### 4.1 MOISTURE TRANSPORT AND 850 hPa AIR DIVERGENCE

Impacts of the surface water and energy budgets of the MP on rainfall changes over Texas are closely linked to corresponding changes in moisture transport and low level air divergence/convergence. Fig. 8 shows differences in 850 hPa specific humidity and horizontal wind between E1 and CTRL during spring and summer. The white areas in Fig. 8 are mountain areas where elevations are greater than 1.5 km. Fig. 9 is the same as Fig. 8 except for the differences between E2 and CTRL. Fig. 10 shows 700 hPa air divergence ( $\text{day}^{-1}$ ) differences between E2 and CTRL during spring and summer. The solid contours represent the air divergence tendency whereas the dashed contours represent the air convergence tendency. The dots represent the areas that pass a student's t-test at the 95% confidence level.

As showed in Fig. 8, in E1, with a drier MP, the lower troposphere water vapor content is slightly lower over the MP and the downstream areas including New Mexico and parts of Texas from March to July. This suggests a dry MP reduces evapotranspiration and results in lower troposphere moisture over the highlands and the downstream regions; decreased moisture suppresses moist convection and hence reduces rainfall. The moisture decrease is most significant in June: the decrease in the 850 hPa specific humidity over New Mexico exceeds  $2 \text{ g kg}^{-1}$ . The water vapor concentration increases over Texas in July and August, indicating that Texas is not downwind of the MP during summer. The geostrophic wind blows along the western flank of the Bermuda High. As the Bermuda high deepens and extends westward from spring to summer, the geostrophic wind changes its direction. As a consequence, over the highlands to the west of Texas, westerlies and northwesterlies prevail during the spring whereas southerlies and southeasterlies prevail during the summer. This feature is well simulated in the

experiments. Wind direction determines the regions affected by the dry air advection from the highlands.

In E2, the heating due to increased absorption of solar radiation depresses the geopotential height over the MP. As a result, a warmer MP is like a “moisture pump” that pushes moist air to the highlands, and this convergence may be further augmented by additional latent heat release during increased precipitation over the MP. Fig. 10 shows a persistent cyclonic flow and increased low level water vapor content over the MP from April to August. The deep warm low drags the LLJ to the highlands, greatly promoting moisture transport over the Sierra Madre Oriental and western Texas. In summer, another deep warm low over Colorado bends the enhanced and northwestward-shifted LLJ northeastward to the central Great Plains. Consequently, as shown in Fig. 9, in summer, anti-cyclonic flow anomalies appear over Texas and air tends to diverge over Texas. As the MP warms up, the temperature gradient between the highlands and the Gulf of Mexico is weaker in spring and hence the prevailing westerly winds weaken (Fig. 9). Consequently, the spring warm air advection effect is not significant in E2.

Fig. 10 shows a summer dipole pattern of air divergence between the MP and the southern US including New Mexico, Texas, and Oklahoma, i.e. low level air tends to converge over the MP whereas it tends to diverge over the southern US. The air divergence tendency is most significant in July and August; it passes a student’s t-test at the 95% confidence level over the southern New Mexico and the western Texas. Therefore, although the enhanced time mean LLJ brings more humid air from the Gulf of Mexico to the southern US from April to August (Fig. 9), rainfall decreases over the southern US during summer (Fig. 14). This result also coincides with the observations (Fig. 3 and 6). If the MP heats up, during summer an enhanced warm low over the MP bend the low-level flow towards the highlands, which is accompanied by an anti-cyclonic

flow and air divergence over the southern US. This circulation response is not favorable for moist convection over Texas. This process is the underlying mechanism that may link the surface temperature of the MP to rainfall over Texas during the summer; it might also be an internal forcing that intensified the 2011 Texas drought. Because the thermal effect tends to dominate the precipitation response, the moisture transport and air divergence between E2 and E3 show little difference. Hence, we do not show the results in E3.

#### **4.2 POTENTIAL TEMPERATURE AND MERIDIONAL WIND SPEED**

To further show the thermal impact of the MP on rainfall over Texas, we also report vertical cross sections of temperature and wind speed in the experiments. Fig. 11 shows the vertical cross sections of potential temperature (K), meridional wind speed ( $\text{m s}^{-1}$ ), and zonal wind ( $\text{m s}^{-1}$ ) along  $30^\circ\text{N}$  from  $120^\circ\text{W}$  to  $80^\circ\text{W}$  in the experiments for spring. The shadings represent potential temperature; the contours show meridional wind speed for CTRL and differences in meridional wind speed between the experiment runs and the control run for E1, E2, and E3; the arrows designate zonal wind for CTRL and differences in zonal wind between the experiment runs and the control run for E1, E2, and E3. Fig.12 is the same as Fig. 11 except that it represents the summer. From Fig. 11 and 12, the meridional speed of the time-mean LLJ does not change noticeably in summer but weakens slightly in spring if the MP dries; it strengthens in spring and summer if the MP heats up, which is consistent with Fig. 9. The time-mean LLJ weakens in spring and strengthens in summer with a warmer and drier MP. The center of the maximum speed of the LLJ is located around  $97^\circ\text{W}$  and 900 hPa in spring; it shifts westward to about  $98^\circ\text{W}$  in summer. The heated MP causes a stronger temperature gradient over the eastern slope of the highlands during summer, which is associated with



the enhanced LLJ, in agreement with Pan et al. (2004). Moreover, Fig. 11 and 12 also show increased air temperature above the MP as the MP warms. In spring, westerly winds prevail in the lower troposphere along 30°N, and the westerlies weaken as air temperatures increase over the MP; in summer, easterly winds prevails in the lower troposphere from 107°W to 95°W, and the easterlies strengthen as air temperatures increase over the MP. The water budget has little influence on the zonal wind speed. In addition, the LLJ over the central and southern plains varies diurnally; this diurnal variation is driven by the thermal wind response to the temperature diurnal variation over the mountain slope (e.g. Holton 1967; Bonner and Paegle 1970). The diurnal feature of LLJ and associated dynamics cannot be reported here because the temporal resolution of our simulation results is monthly.

### **4.3 RAINFALL**

The model results support the spring dry air advection effect and the summer thermodynamic effect of the MP on rainfall over Texas as observed. Fig. 13-15 show the climatological precipitation rate differences among the three experiment runs and the control run in spring and summer. Compared with CTRL, in E1 where we dried the MP, rainfall decreases over most parts of the MP during May, June, and July as shown in Fig. 13. The monthly mean precipitation rate decreases about 1 mm day<sup>-1</sup>, which indicates soil moisture feedbacks on local precipitation over the MP. Dry soils lead to lower evapotranspiration and thus lower latent heat flux into the atmosphere, which is not favorable for convection. We also notice that rainfall decreases over Texas in April and it decreases over New Mexico and western Texas in May and June, which suggests that dry soils over the MP also affect precipitation over downstream areas. Southwesterly winds

blow from the northeastern MP to Texas in April and southerly winds blow from the northern MP to New Mexico and western Texas in May and June. These dry advections suppress precipitation downstream, which conforms with observations shown in Fig. 3 and 5.

Fig. 14 shows that when the MP heats up, rainfall increases significantly over the MP from April to August and rainfall-enhanced areas extend downstream to the central and southern US during spring. Over large portions of the MP, increased precipitation exceeds  $2 \text{ mm day}^{-1}$ . When the MP heats up, a lasting warm low appears over it so that humid air from the surrounding ocean moves to the highlands, which greatly enhances moist convection. During June, rainfall increases over the central MP but decreases over the Sierra Madre del Sur. During July and August, the rainfall-enhanced region spreads over the northern and central MP. The precipitation in July, August, and September accounts for up to 70% of the annual rainfall over the western foothills of the Sierra Madre Occidental (Adams and Comrie, 1997). The rainfall increase over the warmer MP indicates that a warmer MP shifts the primary rainfall areas from the foothills to the highlands. Although rainfall increases over northern Texas in June and over southern Texas in July, it generally decreases throughout the Texas during the summer, especially the western Texas. This result shows that a warmer MP is associated with decreased rainfall over Texas, which is consistent with the observation as shown in Fig. 7 and the low level circulation response as shown in Fig. 9 and 10. Because we dried and warmed the MP in E3, precipitation responds to both the drying and warming effects. However, the rainfall pattern shown in Fig. 15 is similar to Fig. 14, which suggests that the warming effect overshadows the drying effect.

## **Chapter 5: Conclusions**

In this study, we present satellite observations of the 2011 Texas drought, showing that prevailing spring westerly winds brought dry air from the southern Rocky Mountains and the northern MP to Texas. The dry air dehydrated the 700 mb layer over Texas, suppressing convection. The observations indicate that warm dry advection was not significant during the 2011 summer and that the rainfall deficit was not always accompanied by low water vapor content near the surface. However, observational analyses show that a warmer MP is often associated with decreased rainfall over Texas in summer.

Based on hypothesized influences of the MP on rainfall over Texas, we use CESM to further examine how the surface water and energy budgets of the MP affect rainfall over Texas. The results show that reduced soil water content over the MP leads to locally decreased rainfall due to soil moisture-precipitation feedback. Additionally, dry air over MP advects to leeward areas such as Texas in the spring, resulting in a cap inversion that inhibits convection and suppresses the precipitation. A warmer MP heats air over the MP. In summer, a warmer MP serves as a moisture pump that draws the moist air from the foothills to the highlands. Thus, the “moisture pump” tends to favor an anti-cyclonic flow over the southern US, which causes air subsidence over low-elevation areas. This thermal driven circulation induces low-level divergence over the plains and convergence over the altiplano, and hence inhibits convection and tends to decrease rainfall over the southern US, especially over west Texas.

Earth system models cannot explicitly resolve sub-grid scale convection. Mesoscale convective systems contribute to a large amount of precipitation over the southwest (Adams and Comrie, 1997) and quasi-stationary deep convection over the

Great Plains can produce torrential rain (Houze, 2012). Earth system models parameterize these sub-grid scale precipitation processes, so we cannot use Earth system models to study the role of the MP in shaping rainfall over Texas by modulating convection processes. This study focuses on understanding how large-scale circulation response to the prescribed increase of surface solar energy over the MP affects rainfall over Texas. Based on the comparison between model simulations and observations, the moisture transport and 850 hPa air divergence changes discussed in our study are robust, but the rainfall changes, particularly the smaller changes, could be partly attributed to model noise. Moreover, although we make the MP hot in E2, the MP is not dry. The possible reason is that the zero albedo has a larger effect on precipitation than temperature. Increased precipitation over the MP can perturb the middle and upper troposphere circulation. Consequently, the actual circulation response to a warming MP may not be completely consistent with the modeled result.

In addition, to focus on the impact of the MP on rainfall over Texas, we do not allow oceanic feedbacks by prescribing the SST. However, in reality the low-level flow over the southern plains and the Bermuda high are significantly affected by SST variations (e.g. Wang et al. 2007, 2008). Therefore, although this study implies connections between the MP and Texas droughts, we need to bear in mind that a drought generally results from a synthesis of numerous factors such as SST anomalies, anthropogenic global warming, and soil moisture-precipitation feedback (e.g. Hoerling et al. 2013).

	Topography	Albedo	Soil water
Control run (CTRL)	Default	Default	Default
Experiment 1 (E1 DRY)	Default	Default	0.2 mm for each layer
Experiment 2 (E2 WARM)	Default	0	Default
Experiment 3 (E3 DRY & WARM)	Default	0	0.2 mm for each layer

Table 1: Experiments design.

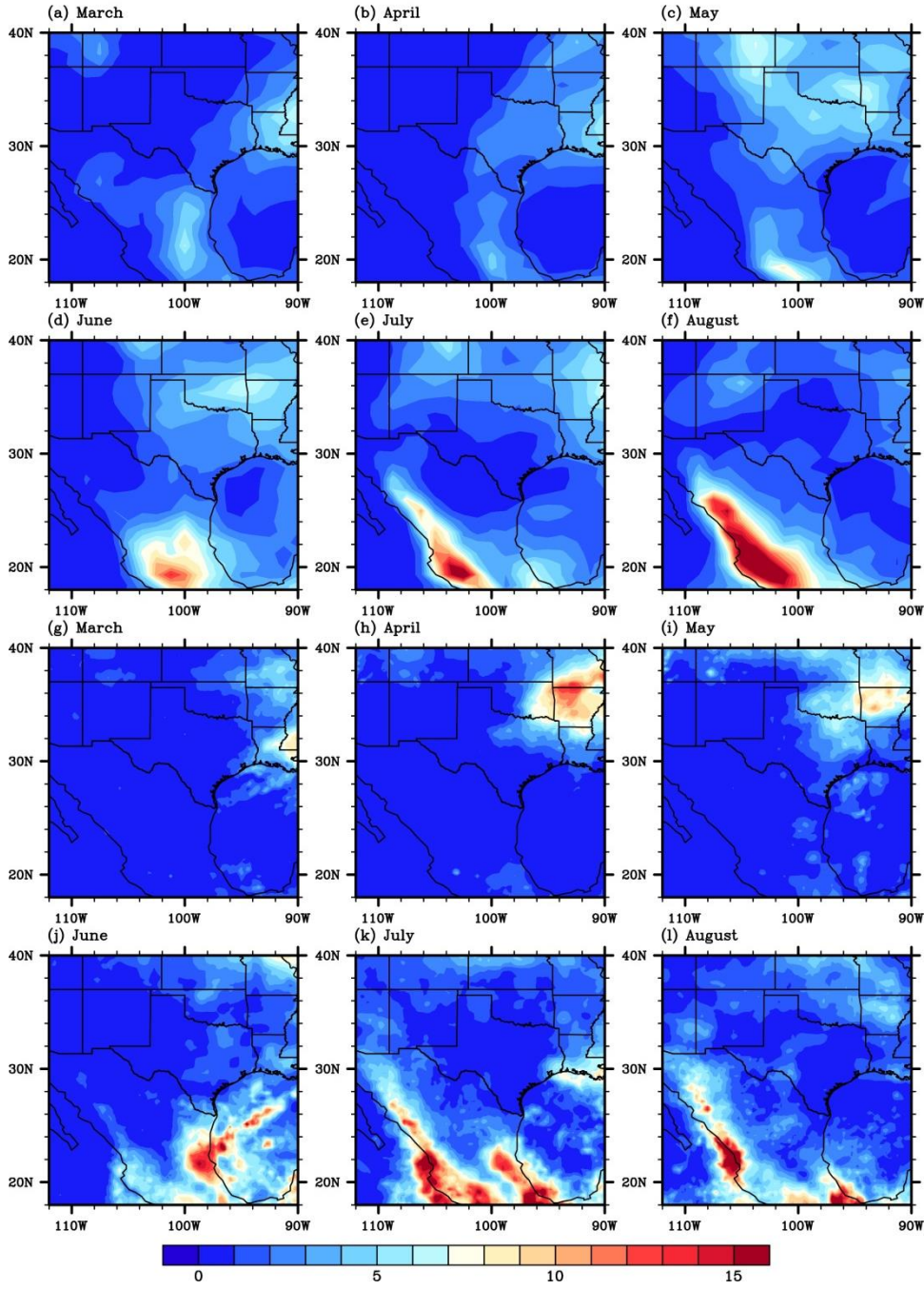


Figure 1: Precipitation rate (mm day<sup>-1</sup>) simulated by CESM (a) – (f) and observed by TRMM (g) – (l) over [112°W, 90°W] × [18°N, 40°N] for the spring and summer of 2011.

850 mb specific humidity (g/kg) and horizontal wind (m/s)

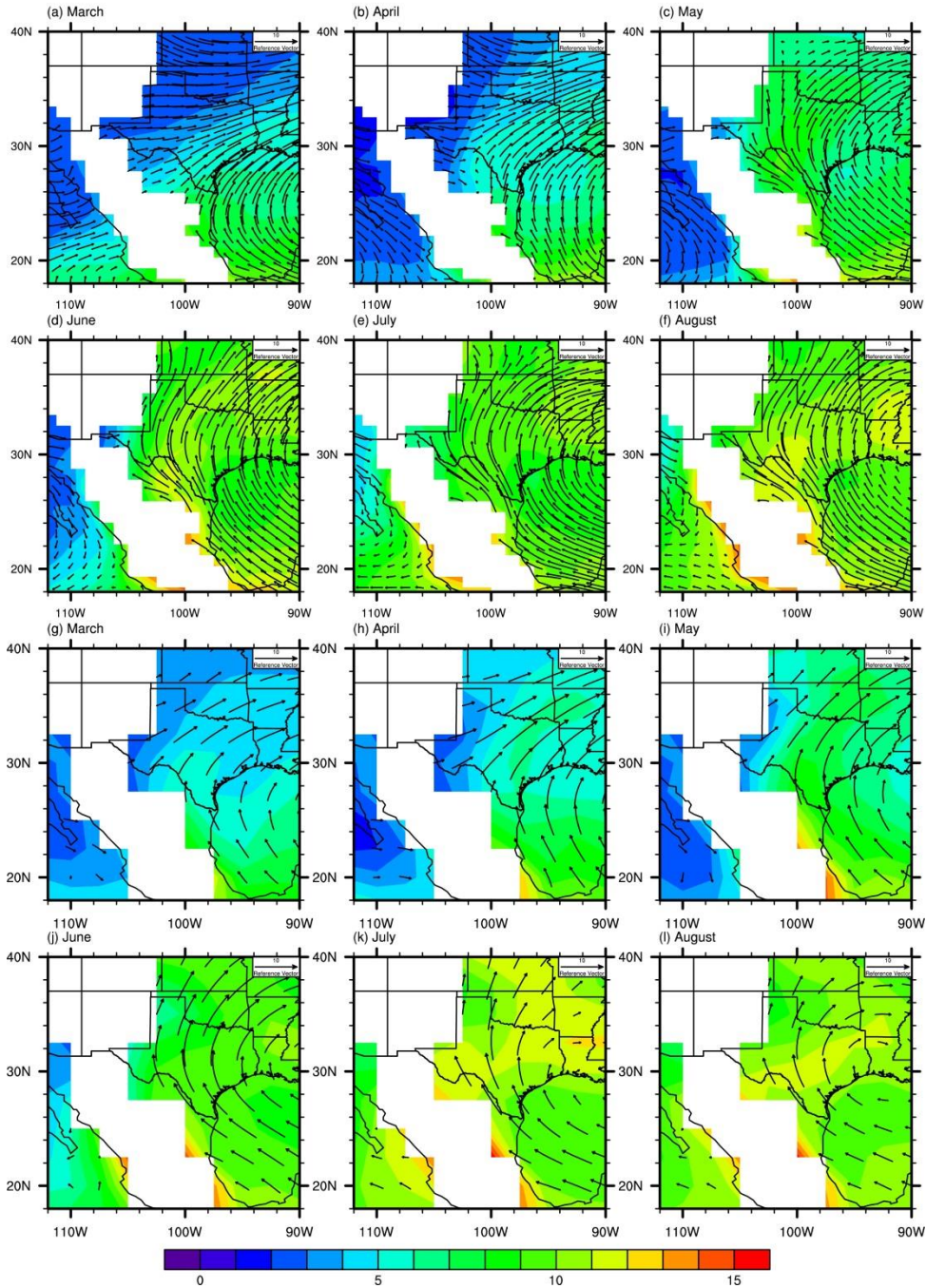


Figure 2: 850 mb specific humidity ( $\text{g kg}^{-1}$ ) and horizontal wind ( $\text{m s}^{-1}$ ) from CESM (a) – (f) and reanalysis (g) – (l) over  $[112^\circ\text{W}, 90^\circ\text{W}] \times [18^\circ\text{N}, 40^\circ\text{N}]$  for the spring and summer of 2011.

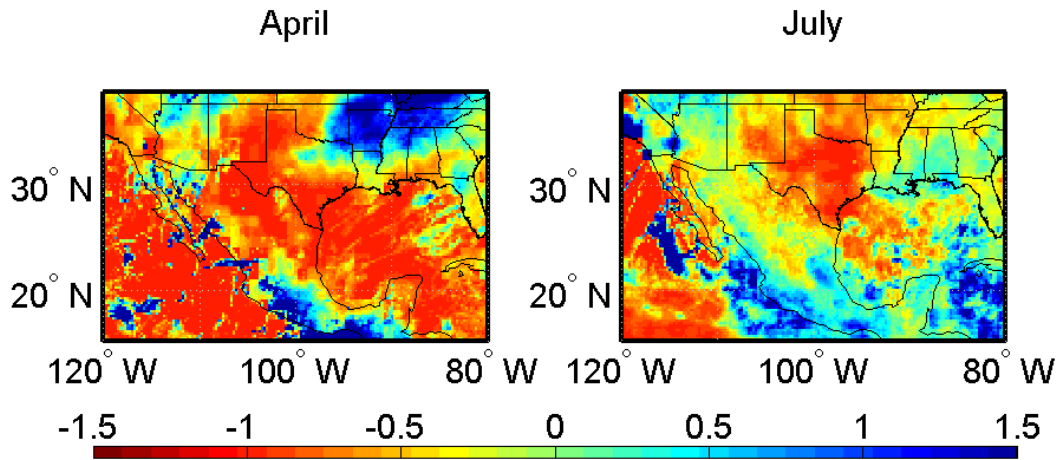


Figure 3: Normalized TRMM 3B43 monthly mean precipitation rate anomalies over  $[120^{\circ}\text{W}, 80^{\circ}\text{W}] \times [15^{\circ}\text{N}, 38^{\circ}\text{N}]$  in April and July of 2011.



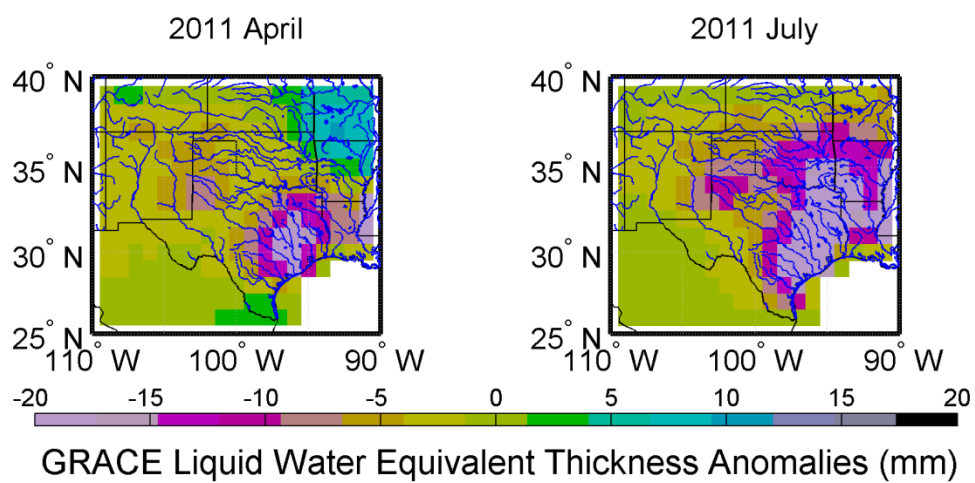


Figure 4: GRACE LWET over the south-central United States in April and July of 2011.

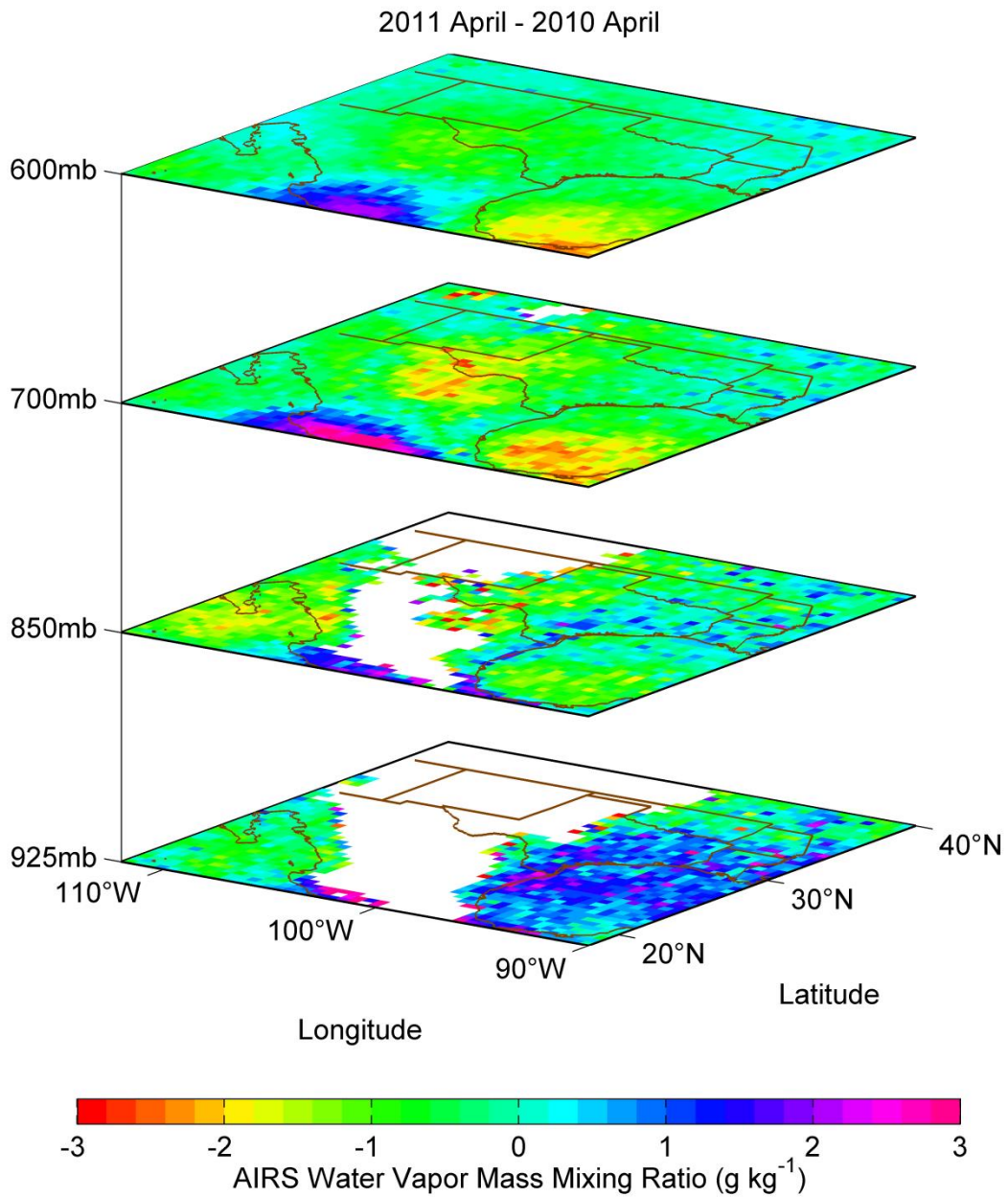


Figure 5: Differences between April 2011 and April 2010 in monthly mean lower and middle troposphere AIRS water vapor mass mixing ratio and NCEP horizontal wind field over the continental US.

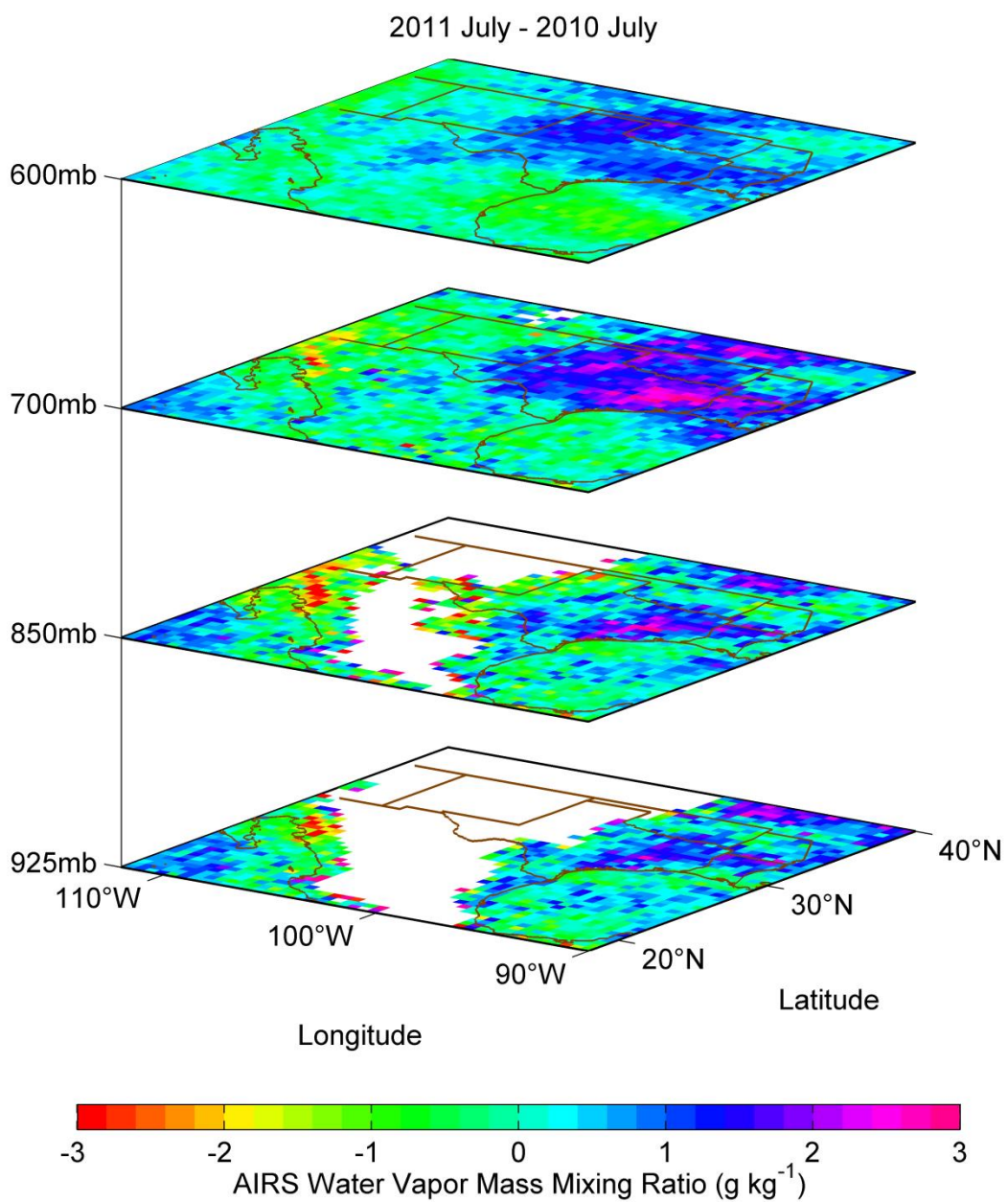


Figure 6: The same as Figure 5 except for the differences between July 2011 and July 2000.

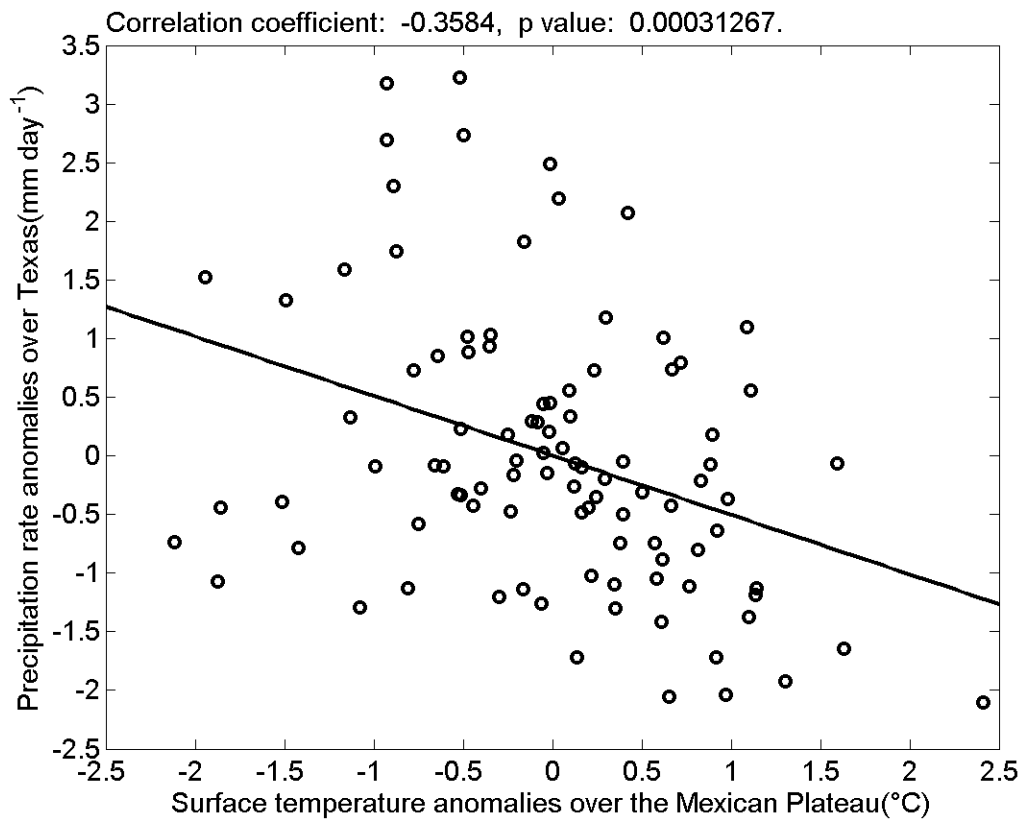


Figure 7: Scatter plot of the precipitation rate anomalies ( $\text{mm day}^{-1}$ ) over Texas and the surface air temperature anomalies ( $^{\circ}\text{C}$ ) of the MP in June, July and August, and the linear regression line.

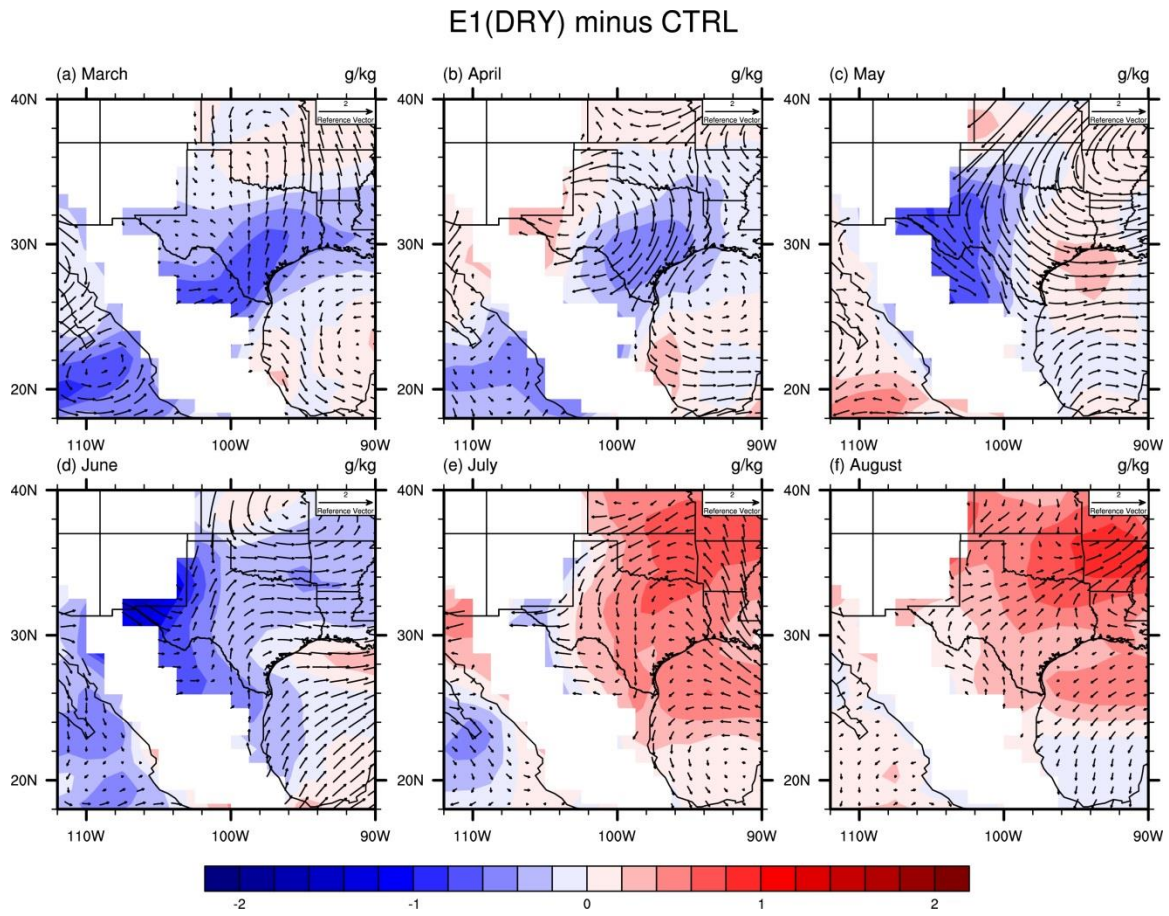


Figure 8: 850 hPa specific humidity ( $\text{g kg}^{-1}$ ) and horizontal wind field differences between E1 and CTRL during spring and summer.



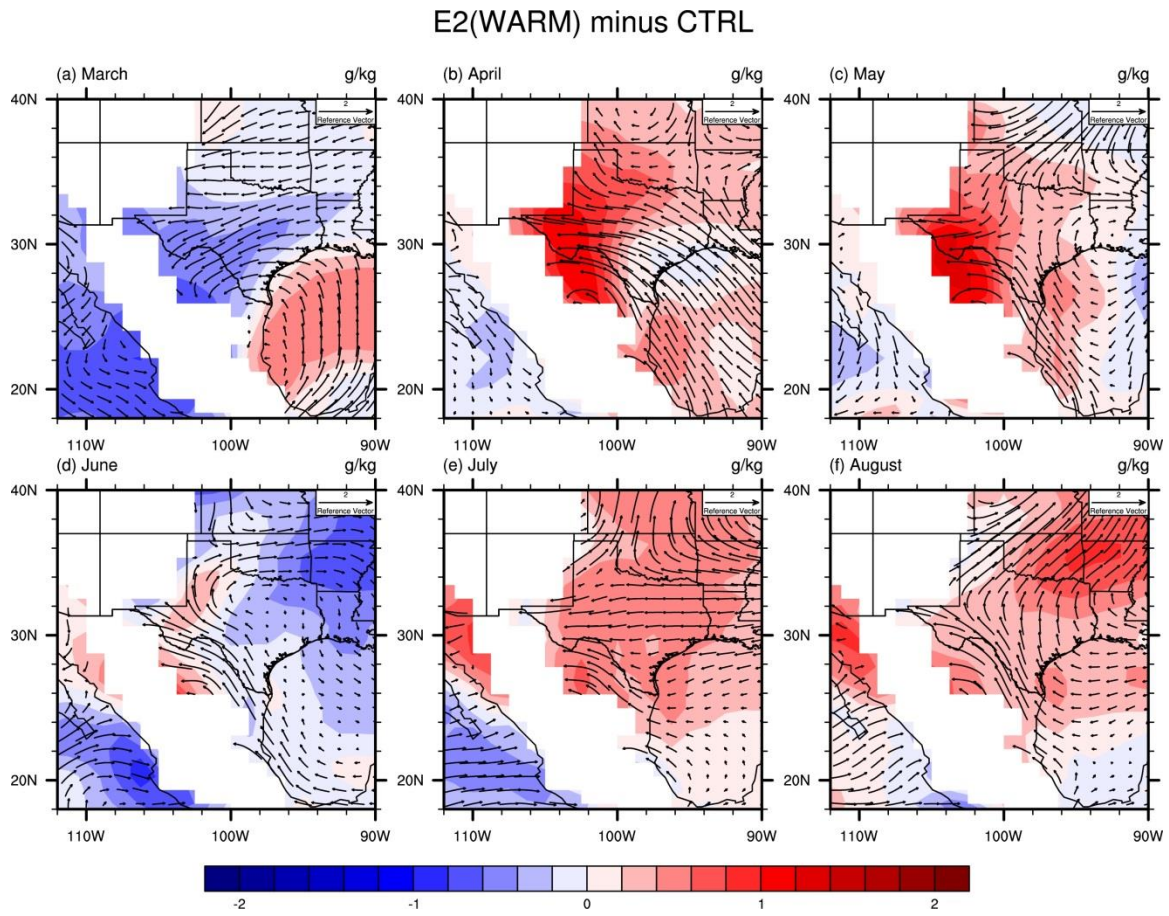


Figure 9: The same as Fig. 8 except for the differences between E2 and CTRL.

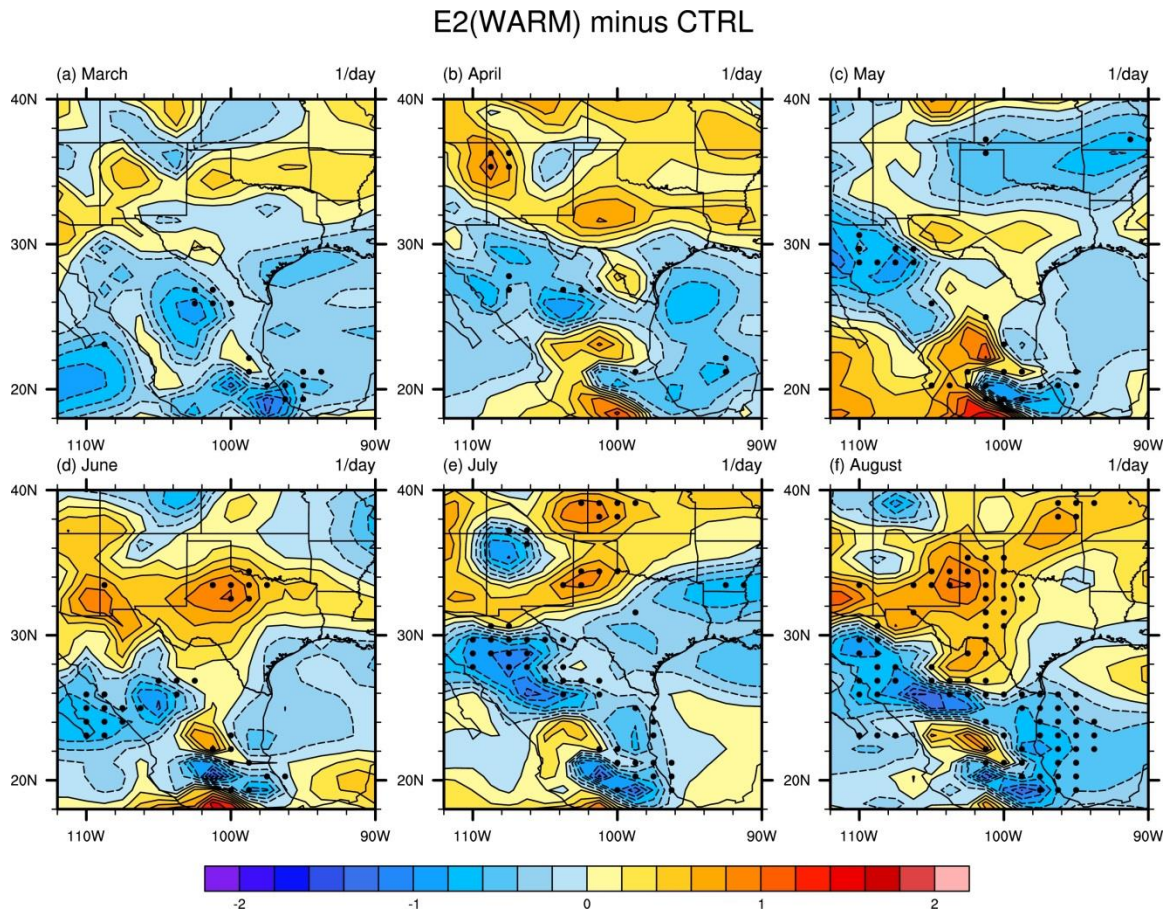


Figure 10: 700 hPa air divergence ( $\text{day}^{-1}$ ) differences between E2 and CTRL during spring and summer. The solid contours represent the air divergence tendency whereas the dashed contours represent the air convergence tendency.

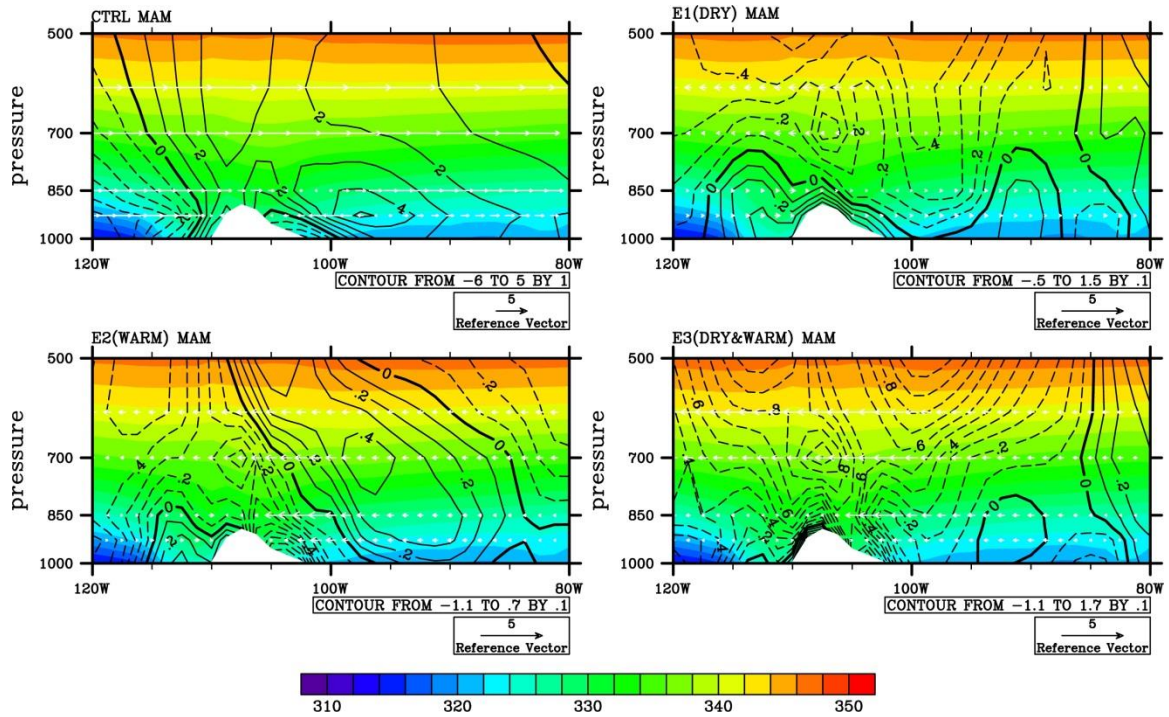


Figure 11: Vertical cross sections of potential temperature (K, shadings), meridional wind ( $\text{m s}^{-1}$ , contours), and zonal wind ( $\text{m s}^{-1}$ , white arrows) along  $30^\circ \text{N}$  from  $120^\circ \text{W}$  to  $80^\circ \text{W}$  for spring (MAM). The contours show meridional wind speed for CTRL and differences in meridional wind speed between the experiment runs and the control run for E1, E2, and E3.



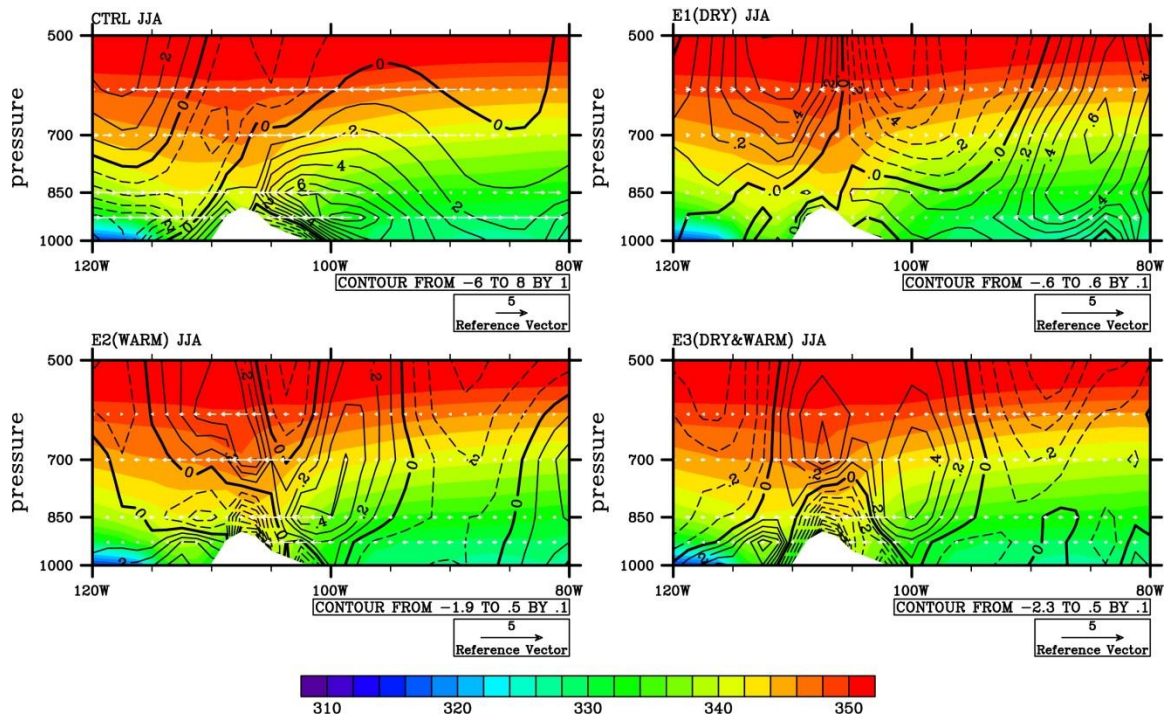


Figure 12: The same as Fig. 11 except for summer (JJA).

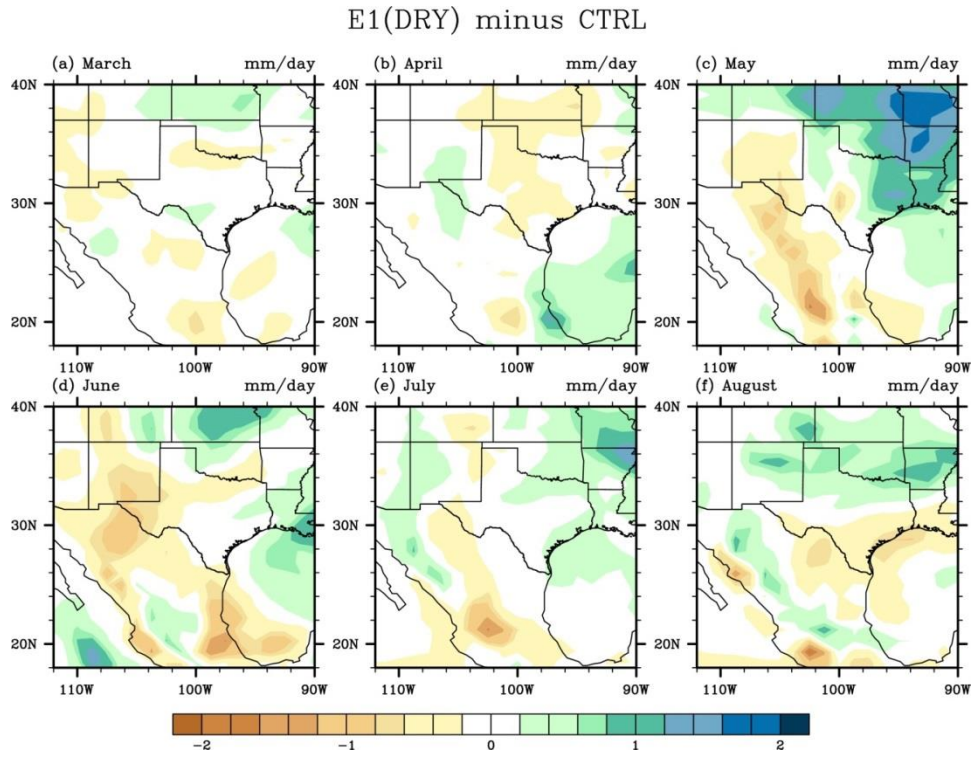


Figure 13: The 2001-2011 mean seasonal precipitation rate (mm/day) differences between E1 and CTRL during spring (March-May) and summer (June-August).

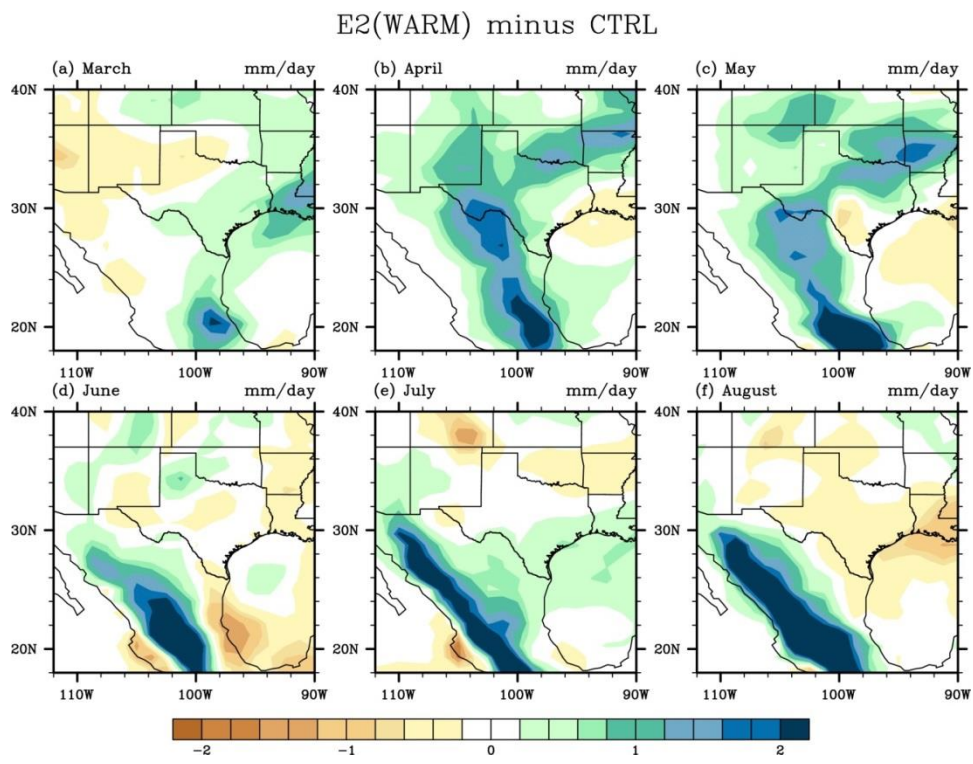


Figure 14: The same as Figure 13 except for the differences between E2 and CTRL.

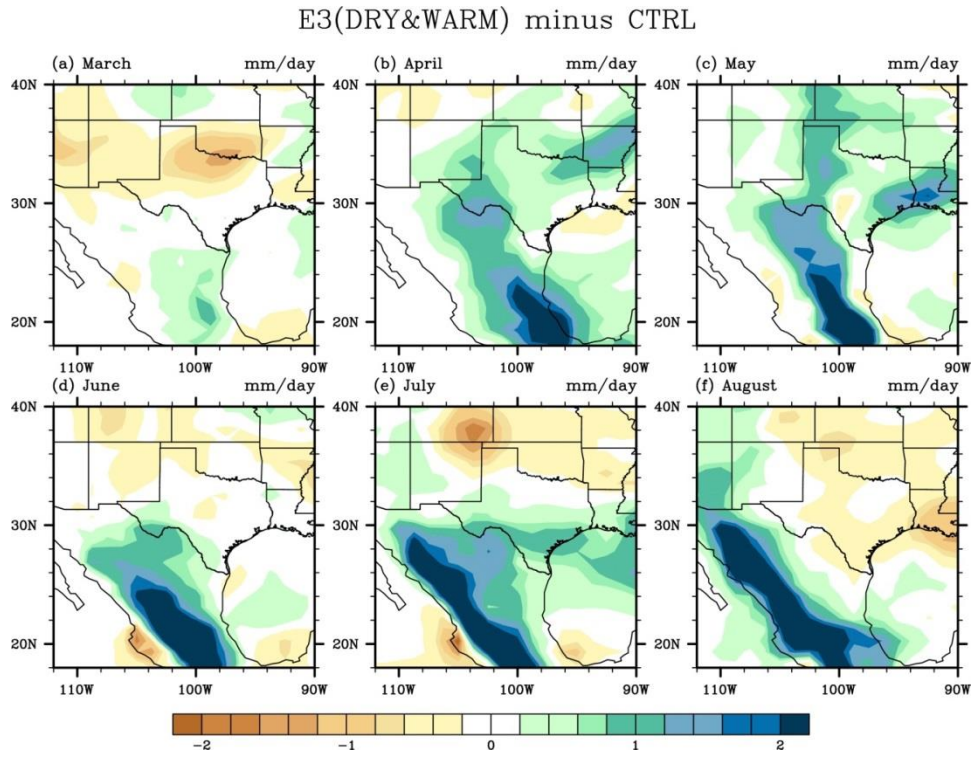


Figure 15: The same as Figure 13 except for the differences between E3 and CTRL.

## References

- Adams, D. K., and A. C. Comrie, 1997: The North American monsoon, *Bull. Amer. Meteor. Soc.*, **78**, 2197-2213.
- Adler, R. F., and Coauthors, 2003: The version-2 global precipitation climatology project (GPCP) monthly precipitation analysis (1979-present). *J. Hydrometeor.*, **4**, 1147-1167.
- Barlow, M., S. Nigam, and E. H. Berbery, 1998: Evolution of the North American monsoon system. *J. Climate*, **11**, 2238-2257.
- Bonner, W. D., and J. Paegle, 1970: Diurnal variations in boundary layer winds over south-central United-States in summer. *Mon. Wea. Rev.*, **98**, 735-744.
- Boos, W. R., and Z. M. Kuang, 2010: Dominant control of the South Asian monsoon by orographic insulation versus plateau heating, *Nature*, **463**, 218-U102.
- Brimelow, J. C., J. M. Hanesiak, and W. R. Burrows, 2011: Impacts of land-atmosphere feedbacks on deep, moist convection on the Canadian prairies, *Earth Interact.*, **15**, doi: 10.1175/2011EI407.1.
- Chepfer, H., S. Bony, D. Winker, M. Chiriaco, J. L. Dufresne, and G. Seze, 2008: Use of CALIPSO lidar observations to evaluate the cloudiness simulated by a climate model. *Geophys. Res. Lett.*, **35**.
- Cook, K. H., and E. K. Vizy, 2010: Hydrodynamics of the Caribbean low-level jet and its relationship to precipitation, *J. Climate*, **23**, 1477-1494.
- Dai, A., 2013: The influence of the inter-decadal Pacific oscillation on US precipitation during 1923–2010, *Clim. Dyn.*, **41**, 633-646.
- Dirmeyer, P. A., 1994: Vegetation stress as a feedback mechanism in midlatitude drought, *J. Climate*, **7**, 1463-1483.
- Hoerling, M., and Coauthors, 2013: Anatomy of an Extreme Event. *J. Climate*, **26**, 2811-2832.
- Holton, J. R., 1967: Diurnal boundary layer and oscillation above sloping terrain. *Tellus*, **19**, 199-205.
- Houze, R. A., 2012: Orographic effects on precipitating clouds, *Rev. Geophys.*, **50**, RG1001.
- Hurrell, J. W., et al. (2013), The Community Earth System Model A Framework for Collaborative Research, *Bull. Amer. Meteor. Soc.*, **94**, 1339-1360.
- Kalnay, E., and Coauthors, 1996: The NCEP/NCAR 40-year reanalysis project. *Bull. Amer. Meteor. Soc.*, **77**, 437-471.
- Klein, S. A., and C. Jakob, 1999: Validation and sensitivities of frontal clouds simulated by the ECMWF model. *Mon. Wea. Rev.*, **127**, 2514-2531.

- Koster, R. D., and Coauthors, 2004: Regions of strong coupling between soil moisture and precipitation, *Science*, **305**, 1138-1140.
- Landerer, F. W., and S. C. Swenson, 2012: Accuracy of scaled GRACE terrestrial water storage estimates, *Water Resour. Res.*, **48**, W04531.
- Lau, N.-C., A. Leetmaa, and M. J. Nath, 2008: Interactions between the responses of North American climate to El Niño–La Niña and to the secular warming trend in the Indian–Western Pacific Oceans, *J. Climate*, **21**, 476-494.
- Li, L. F., W. H. Li, and Y. Kushnir, 2012: Variation of the North Atlantic subtropical high western ridge and its implication to Southeastern US summer precipitation, *Clim. Dyn.*, **39**, 1401-1412.
- Menon, S., 2002: Climate effects of black carbon aerosols in China and India, *Science*, **297**, 2250-2253.
- Mo, K. C., and E. H. Berbery, 2004: Low-level jets and the summer precipitation regimes over North America, *J. Geophys. Res.*, **109**, D06117.
- , J. K. E. Schemm, and S. H. Yoo, 2009: Influence of ENSO and the Atlantic Multidecadal Oscillation on drought over the United States, *J. Climate*, **22**, 5962-5982.
- Myoung, B., and J. W. Nielsen-Gammon, 2010: The convective instability pathway to warm season drought in Texas. Part II: free-tropospheric modulation of convective inhibition, *J. Climate*, **23**, 4474-4488.
- Pan, Z. T., M. Segal, and R. W. Arritt, 2004: Role of topography in forcing low-level jets in the Central United States during the 1993 flood-altered terrain simulations, *Mon. Wea. Rev.*, **132**, 396-403.
- Seager, R., L. Goddard, J. Nakamura, N. Henderson, and D. Lee, 2013: Dynamical causes of the 2010/11 Texas-northern Mexico drought, *J. Hydrometeor.*, in press.
- Stensrud, D. J., 1996: Importance of low-level jets to climate: A review, *J. Climate*, **9**, 1698-1711.
- Tang, M. C., and E. R. Reiter, 1984: Plateau monsoons of the northern hemisphere – a comparison between North-America and Tibet, *Mon. Wea. Rev.*, **112**, 617-637.
- Ting, M. F., and H. L. Wang, 2006: The role of the North American topography on the maintenance of the great plains summer low-level jet, *J. Atmos. Sci.*, **63**, 1056-1068.
- Wang, C. Z., S. K. Lee, and D. B. Enfield, 2007: Impact of the Atlantic warm pool on the summer climate of the Western Hemisphere, *J. Climate*, **20**, 5021-5040.
- , 2008: Climate response to anomalously large and small Atlantic warm pools during the summer. *J. Climate*, **21**, 2437-2450.

- Zhang, T., M. P. Hoerling, J. Perlwitz, D. Z. Sun, and D. Murray, 2011: Physics of US surface temperature response to ENSO, *J. Climate*, **24**, 4874-4887.
- Zhao, C., X. Liu, and L. R. Leung, 2012: Impact of the Desert dust on the summer monsoon system over Southwestern North America, *Atmos. Chem. Phys.*, **12**, 3717-3731.